Research Article

Naveed Iqbal, Mohammad Alqudah, Yousef Jawarneh, Ahmad Shafee, Ali M. Mahnashi, and Fazal Ghani*

Novel analysis of fractional regularized long-wave equation in plasma dynamics

https://doi.org/10.1515/phys-2025-0182
received July 17, 2024; accepted June 26, 2025

Abstract: In this study, we investigate the fractional regularized long-wave (FRLW) equation using the Aboodh transform iteration method (ATIM), a semi-analytical technique that effectively combines the Aboodh integral transform with iterative schemes to handle fractional differential equations. The FRLW equation, a nonlinear model arising in ion-acoustic wave propagation in plasma, is extended to the fractional domain to better capture the temporal nonlocal behavior. The proposed method provides approximate analytical solutions in a straightforward and computationally efficient manner. Graphical results are presented to demonstrate the impact of the fractional-order parameter on wave dynamics, including dispersion and stability. The results confirm that ATIM is a powerful and accurate approach for solving nonlinear fractional partial differential equations and enriches the analytical understanding of fractional plasma wave models.

Keywords: Aboodh transform iteration method, regularized long-wave equations, fractional-order PDE, Caputo operator

*** Corresponding author: Fazal Ghani,** Department of Mathematics, Abdul Wali Khan University, Mardan 23200, Pakistan, e-mail: fghanimath@awkum.edu.pk
Naveed Iqbal: Department of Mathematics, College of Science, University of Ha'il, Ha'il 2440, Saudi Arabia, e-mail: n.iqbal@uoh.edu.sa
Mohammad Alqudah: Department of Basic Sciences, School of Electrical Engineering & Information Technology, German Jordanian University, Amman, 11180, Jordan, e-mail: mohammad.qudah@gju.edu.jo
Yousef Jawarneh: Department of Mathematics, College of Science, University of Ha'il, Ha'il 2440, Saudi Arabia, e-mail: y.jawarneh@uoh.edu.sa
Ahmad Shafee: PAAET, College of Technological Studies, Laboratory Technology Department, Shuwaikh 70654, Kuwait, e-mail: as.zada@paaet.edu.kw
Ali M. Mahnashi: Department of Mathematics, College of Science, Jazan University, Jazan, Saudi Arabia, e-mail: amahnashi@jazanu.edu.sa

1 Introduction

Fractional differential equations (FDEs) and fractional calculus have lately attracted interest among mathematicians, physicists, and engineers. Materials engineering, electromagnetic, viscoelastic, electrochemistry, and dynamical physics are among the scientific and technical fields represented using fractional partial differential equations (FPDEs). Many important implementations in several fields have been evaluated [1]. Analytic solutions of FDEs are really fascinating. Approaches of linearization or series solution, discretization [2–4], and system solvers [5–7] must be applied in order to obtain approximation techniques. Non-linear events are addressed in many disciplines of engineering and study. These cover chemical kinetics, solid-state physics, computational biology, quantum mechanics, fluid physics, non-linear spectroscopy, thermodynamics, and many more [8–12]. The theory of non-linearity finds roots in these higher-order nonlinear partial differential equations. All physical systems can be understood nonlinearly [13,14].

In this work, the regularized long wave equations are solved using the Aboodh transform iterative method (ATIM).

The time-fractional nonlinear regularized long wave (RLW) equation is given as [15]

$$D_{\nu}^{p}\Omega(\mu,\nu) = \frac{\partial^{3}\Omega(\mu,\nu)}{\partial\nu\partial\mu^{2}} - \frac{1}{2}\frac{\partial\Omega^{2}(\mu,\nu)}{\partial\mu}, \tag{1}$$

with initial condition

$$\Omega(\mu,0) = \mu. \tag{2}$$

The time-fractional nonlinear generalized GRLW equation is defined as [15]

$$D_{\nu}^{p}\Omega(\mu,\nu) = \frac{\partial^{3}\Omega(\mu,\nu)}{\partial\nu\partial\mu^{2}} - \Omega(\mu,\nu)\frac{\partial\Omega(\mu,\nu)}{\partial\mu} - \frac{\partial\Omega(\mu,\nu)}{\partial\mu}, \tag{3}$$

with initial condition:

$$\Omega(\mu,0) = 3k\,\mathrm{sech}^{2}(l\mu), \tag{4}$$

The time-fractional linear regularized long wave (RLW) equation [15]

$$D_v^p \Omega(\mu, v) = 2\frac{\partial^3 \Omega(\mu, v)}{\partial v \partial \mu^2} - \frac{\partial \Omega(\mu, v)}{\partial \mu}, \tag{5}$$

with initial condition:

$$\Omega(\mu, 0) = e^{-\mu}. \tag{6}$$

The time-fractional linear RLW equation [15]

$$D_v^p \Omega(\mu, v) = -\frac{\partial^4 \Omega(\mu, v)}{\partial \mu^4}, \tag{7}$$

with initial condition:

$$\Omega(\mu, 0) = \sin(\mu). \tag{8}$$

The first equation is called the regularized long wave equation (RLWE), the second equation is called the general regularized long wave GRLWE equation both of them are nonlinear, and the third and fourth equations are called linear regularized long wave equations (RLWEs) [15].

This equation is an updated form of the Korteweg–de Vries equation for the modeling of surface gravity waves with modest amplitudes that propagate in two dimensions. RLW equations find application in some scientific domains for things such as longitudinal dispersive waves, rotating tube flow, ion-acoustic, magneto-hydrodynamic waves in plasma, stress waves in compressed gas bubble mixtures, and other kinds of situations [16–20]. Considered as basic models in the domains of engineering and applied physics, the RLW equations can help to depict many significant physical structures. Regarding viscous or shock waves, flow problems, diffusion is among the several situations that arise. It is relevant for the modeling of dissipation-oriented non-linear wave diffusion problems. Though it all depends on the issue model [21], this dissipation may cause heat conduction, chemical reaction, viscosity, mass diffusion, thermal radiation, or any other thing.

Excellent models for forecasting real-world events are produced by the RLW problem, a subtype of growth models. Initially, the oscillating bearing behavior was supposed to be distinguished by including the algorithm [22]. It was also produced via investigation on ions and acoustic plasma waves in water. Analytically under initial condition and boundary condition, a solution to the RLW problem was developed in the study by Benjamin et al. [23]. In ocean engineering and research, fractional RLW equations explain several significant events, including long-wave phenomena and shallow water waves of small frequency. Several researchers find significant fascination in ocean shallow waves of liquid; non-linear waves modeled on the fractional equations of RLW especially appeal to them. Mathematical models of the ocean non-linear waves were embodied by the RLW equations. Actually, fractional RLW equations define the massive surface waves called tsunamis. Using the current very efficient method, fractional RLW equations, the enormous internal waves in the ocean's deep might be developed that would destroy marine ships due to temperature variations.

In the past few decades, scientists and researchers have created and employed a number of analytical techniques to tackle these kinds of issues. The variational iteration method (VIM), homotopy perturbation method (HPM) [24], the least-squares method [25], the Adomian decomposition method [26,27], the He's HPM [28], and the homotopy perturbation Sumudu transform method (HPSTM) [15] are a few of these techniques. Some of the limitations of these approaches that have been noted are the computation of Adomian polynomials, the determination of the Lagrange multiplier, diverging findings, and a large number of computations.

The ATIM, one of the most important mathematical innovations, can be used to solve FPDEs. Conventional methods for resolving FPDEs can be computationally costly and cause problems with convergence. Our innovative approach obtains around these limitations by continuously improving approximations while maintaining a stable computational economy. This allows us to continuously enhance accuracy. This finding improves our ability to recognize and comprehend complicated systems driven by FPDEs, which in turn helps to solve challenging issues in physics, engineering, and applied mathematics [29–31].

The simplest basic method for solving FDEs is the ATIM, according to previous studies [29–31]. These methods not only yield numerical solutions to PDEs that do not require discretization, but they also immediately and clearly reveal the symbolic terms in analytical solutions. The main goal of this work is to evaluate how well ATIM solves the acoustic wave equations. It is important to note that these two methods have been used to solve a number of linear and nonlinear fractional differential problems.

The study of ion-acoustic plasma waves is fundamental in understanding various phenomena in space and laboratory plasmas. Traditional models, such as the RLW equation, have been instrumental in describing wave propagation and dispersion in such media. However, these models often fail to account for memory effects and nonlocal interactions that are intrinsic to many complex physical systems, particularly in plasmas with long-range particle interactions. Fractional calculus, especially using the Caputo derivative, provides a powerful framework to incorporate these effects due to its ability to model temporal and spatial memory. In this work, we employ the ITM to derive approximate analytical solutions of the fractional RLW equation. The fractional-order formulation allows for a deeper understanding of the impact of memory and

nonlocality on wave dynamics. Our findings not only generalize the classical RLW model but also offer new insights into the role of fractional parameters in controlling the stability and dispersive behavior of plasma waves.

2 Foundations of our work

Definition 2.1. [32] Aboodh transform (AT) is defined as follows for the piecewise continuous and exponential order function $\Omega(\mu, \nu)$:

$$A[\Omega(\mu,\nu)] = \Psi(\mu,\xi) = \frac{1}{\xi}\int_0^\infty \Omega(\mu,\nu)e^{-\nu\xi}\mathrm{d}\nu,$$
$$\sigma_1 \le \xi \le \sigma_2 \quad \text{and} \quad \mu \ge 0.$$

The inverse transform of Aboodh (IAT) is given as

$$A^{-1}[\Psi(\mu,\xi)] = \Omega(\mu,\nu) = \frac{1}{2\pi i}\int_{u-i\infty}^{u+i\infty}\Psi(\mu,\nu)\xi e^{\nu\xi}\mathrm{d}\nu,$$
$$\mu = (\mu_1, \mu_2, \ldots, \mu_p) \in \mathbb{R} \quad \text{and} \quad p \in \mathbb{N}.$$

Lemma 2.1. [33,34] *Consider two piecewise continuous and exponential-order functions $\Omega_1(\mu,\nu)$ and $\Omega_2(\mu,\nu)$ on $[0,\infty[$. Let $A[\Omega_1(\mu,\nu)] = \Psi_1(\mu,\nu)$, $A[\Omega_2(\mu,\nu)] = \Psi_2(\mu,\nu)$, and constants ϱ_1 and ϱ_2. Consequently, these features are sufficient:*

(*i*) $A[\varrho_1\Omega_1(\mu,\nu) + \varrho_2\Omega_2(\mu,\nu)] = \varrho_1\Psi_1(\mu,\xi) + \varrho_2\Psi_2(\mu,\nu)$,

(*ii*) $A^{-1}[\varrho_1\Psi_1(\mu,\nu) + \varrho_2\Psi_2(\mu,\nu)] = \varrho_1\Omega_1(\mu,\xi) + \varrho_2\Omega_2(\mu,\nu)$,

(*iii*) $A[J_\nu^p\Omega(\mu,\nu)] = \frac{\Psi(\mu,\xi)}{\xi^p}$,

(*iv*) $A[D_\nu^p\Omega(\mu,\nu)] = \xi^p\Psi(\mu,\xi) - \sum_{r=0}^{l-1}\frac{\Omega^r(\mu,0)}{\xi^{r-p+2}}$, $l-1 < p \le l$, $\quad l \in \mathbb{N}$.

Definition 2.2. [35] The fractional Caputo derivative of order p for the function $\Omega(\mu,\nu)$ is stated as

$$D_\nu^p\Omega(\mu,\nu) = J_\nu^{n-p}\Omega^{(n)}(\mu,\nu), \quad l \ge 0, \quad n-1 < p \le n,$$
$$n, p \in \mathbb{R}, J_\nu^{n-p} \text{ is the R–L integral of } \Omega(\mu,\nu).$$

Definition 2.3. [36] Power series of the multiple fractional (PSMF) is given as

$$\sum_{l=0}^{\infty}\hbar_l(\mu)(\nu-\nu_0)^{lp} = \hbar_0(\nu-\nu_0)^0 + \hbar_1(\nu-\nu_0)^p + \hbar_2(\nu-\nu_0)^{2p} + \ldots,$$

where $\mu = (\mu_1, \mu_2, \ldots, \mu_p) \in \mathbb{R}^p$ and $p \in \mathbb{N}$, ν is variable, the series coefficients $\hbar_l(\mu)$, and the series is centered about ν_0.

Lemma 2.2. *Let us consider that there exist exponential-order function $\Omega(\mu,\nu)$ and define AT as $A[\Omega(\mu,\nu)] = \Psi(\mu,\xi)$. Then,*

$$A[D_\nu^{lp}\Omega(\mu,\nu)] = \xi^{lp}\Psi(\mu,\xi) - \sum_{j=0}^{l-1}\xi^{p(l-j)-2}D_\nu^{jp}\Omega(\mu,0), \quad 0 < p \le 1, \tag{9}$$

where $\mu = (\mu_1, \mu_2, \ldots, \mu_p) \in \mathbb{R}^p$ and $p \in \mathbb{N}$ and $D_\nu^{lp} = D_\nu^p.\ D_\nu^p.\ \ldots.\ D_\nu^p (l - times)$.

Proof. Eq. (9) can be verified by the process of induction. By substituting $l = 1$ into Eq. (9), the following is obtained:

$$A[D_\nu^{2p}\Omega(\mu,\nu)] = \xi^{2p}\Psi(\mu,\xi) - \xi^{2p-2}\Omega(\mu,0) - \xi^{p-2}D_\nu^p\Omega(\mu,0).$$

The validity of Eq. (9) is asserted by Lemma 2.1 for $l = 1$. This result is obtained when $l = 2$ is inserted into Eq. (9):

$$A[D_l^{2p}\Omega(\mu,\nu)] = \xi^{2p}\Psi(\mu,\xi) - \xi^{2p-2}\Omega(\mu,0) - \xi^{p-2}D_\nu^p\Omega(\mu,0). \tag{10}$$

The left-hand side (LHS) of Eq. (10) will allow us to achieve this result:

$$\text{L.H.S} = A[D_\nu^{2p}\Omega(\mu,\nu)]. \tag{11}$$

Eq. (11) can also be expressed as

$$\text{L.H.S} = A[D_\nu^p\Omega(\mu,\nu)]. \tag{12}$$

Let

$$Z(\mu,\nu) = D_\nu^p\Omega(\mu,\nu). \tag{13}$$

Thus, Eq. (12) becomes

$$\text{L.H.S} = A[D_\nu^p z(\mu,\nu)]. \tag{14}$$

Using Definition 2.2, we can rewrite Eq. (14) as

$$\text{L.H.S} = A[J^{1-p}z'(\mu,\nu)]. \tag{15}$$

The Riemann-Liouville integral for the AT is applied to Eq. (15), resulting in the following:

$$\text{L.H.S} = \frac{A[z'(\mu,\nu)]}{\xi^{1-p}}. \tag{16}$$

By virtue of the derivative characteristic of the AT, Eq. (16) is transformed

$$\text{L.H.S} = \xi^p Z(\mu,\xi) - \frac{z(\mu,0)}{\xi^{2-p}}. \tag{17}$$

From Eq. (13), we derive

$$Z(\mu,\xi) = \xi^p\Psi(\mu,\xi) - \frac{\Omega(\mu,0)}{\xi^{2-p}}.$$

Substitute the value of $Z(\mu, \xi)$ into Eq. (17):

$$\text{L.H.S} = \xi^{2p}\Psi(\mu, \xi) - \frac{\Omega(\mu, 0)}{\xi^{2-2p}} - \frac{D_v^p\Omega(\mu, 0)}{\xi^{2-p}}. \tag{18}$$

Eq. (9) is valid when $l = r$. In Eq. (9), substitute $l = r$:

$$A[D_v^{rp}\Omega(\mu, v)] = \xi^{rp}\Psi(\mu, \xi) - \sum_{j=0}^{r-1}\xi^{p(r-j)-2}D_v^{jp}D_v^{jp}\Omega(\mu, 0), \quad 0 < p \le 1. \tag{19}$$

Ultimately, we must demonstrate that Eq. (9) is valid for $l = r + 1$ by inserting it into Eq. (9):

$$A[D_v^{(r+1)p}\Omega(\mu, v)] = \xi^{(r+1)p}\Psi(\mu, \xi) - \sum_{j=0}^{r}\xi^{p((r+1)-j)-2}D_v^{jp}\Omega(\mu, 0). \tag{20}$$

We derive the following after analyzing the LHS of Eq. (20):

$$\text{L.H.S} = A[D_v^{rp}(D_v^{rp})]. \tag{21}$$

Let

$$D_v^{rp} = g(\mu, v).$$

By Eq. (21), we drive

$$\text{L.H.S} = A[D_v^p g(\mu, v)]. \tag{22}$$

The Riemann-Liouville integral to Eq. (22) and the definition 2.2 provide the following:

$$\text{L.H.S} = \xi^p A[D_v^{rp}\Omega(\mu, v)] - \frac{g(\mu, 0)}{\xi^{2-p}}. \tag{23}$$

Eq. (19) is employed to obtain Eq. (23):

$$\text{L.H.S} = \xi^{lp}\Psi(\mu, \xi) - \sum_{j=0}^{l-1}\xi^{p(l-j)-2}D_v^{jp}\Omega(\mu, 0). \tag{24}$$

Eq. (24) can also be expressed as

$$\text{L.H.S} = A[D_v^{l+p}\Omega(\mu, 0)].$$

Eq. (9) is therefore valid when $l = r + 1$. Hence, it is proved that Eq. (9) is valid for all positive integers by mathematical induction. □

The lemma that follows provides a novel explanation of multiple fractional Taylor's series (MFTS). This formula will be advantageous to the Aboodh residual power series method (which will be further examined in the following).

Lemma 2.3. *Assume that $\Omega(\mu, v)$ be the function of exponential order. The AT of $\Omega(\mu, v)$ is denoted by the expression $A[\Omega(\mu, v)] = \Psi(\mu, \xi)$. Then, the MFTS in the AT is denoted as*

$$\Psi(\mu, \xi) = \sum_{l=0}^{\infty}\frac{\hbar_l(\mu)}{\xi^{lp+2}}, \xi > 0, \tag{25}$$

where $\mu = (\mu_1, \mu_2, ..., \mu_p) \in \mathbb{R}^p, \quad p \in \mathbb{N}$.

Proof. Consider Taylor's series:

$$\Omega(\mu, v) = \hbar_0(\mu) + \hbar_1(\mu)\frac{v^p}{\Gamma[p+1]} + + \hbar_2(\mu)\frac{v^{2p}}{\Gamma[2p+1]} + ... \tag{26}$$

The following is the result of applying the AT to Eq. (26):

$$A[\Omega(\mu, v)] = A[\hbar_0(\mu)] + A\left[\hbar_1(\mu)\frac{v^p}{\Gamma[p+1]}\right] + A\left[\hbar_1(\mu)\frac{v^{2p}}{\Gamma[2p+1]}\right] + ...$$

When implemented, the transformation generates the consequent output

$$A[\Omega(\mu, v)] = \hbar_0(\mu)\frac{1}{\xi^2} + \hbar_1(\mu)\frac{\Gamma[p+1]}{\Gamma[p+1]}\frac{1}{\xi^{p+2}} + \hbar_2(\mu)\frac{\Gamma[2p+1]}{\Gamma[2p+1]}\frac{1}{\xi^{2p+2}} ...$$

Following a set of calculations, we obtain Eq. (25), a novel specific form of Taylor's series in the AT. □

Lemma 2.4. *The PSMF in the Taylor series* (25) *formulation is as follows*: $A[\Omega(\mu, v)] = \Psi(\mu, \xi)$.

$$\hbar_0(\mu) = \lim_{\xi\to\infty}\xi^2\Psi(\mu, \xi) = \Omega(\mu, 0). \tag{27}$$

Proof. Assume Taylor's series:

$$\hbar_0(\mu) = \xi^2\Psi(\mu, \xi) - \frac{\hbar_1(\mu)}{\xi^p} - \frac{\hbar_2(\mu)}{\xi^{2p}} - ... \tag{28}$$

With a brief computation, we can obtain (28) by calculating $\lim_{\xi\to\infty}$ of Eq. (27). □

Theorem 2.5. *In the AT, the PSMF for the function $\Omega(\mu, v)$ is as follows.*

$$\Psi(\mu, \xi) = \sum_{l=0}^{\infty}\frac{\hbar_l(\mu)}{\xi^{lp+2}}, \quad \xi > 0,$$

where $\mu = (\mu_1, \mu_2, ..., \mu_p) \in \mathbb{R}^p$ and $p \in \mathbb{N}$. Then, we have

$$\hbar_l(\mu) = D_r^{lp}\Omega(\mu, 0),$$

where, $D_v^{lp} = D_v^p.\ D_v^p.\ ....\ D_v^p(l - times)$.

Proof. Assume Taylor's series:

$$\hbar_1(\mu) = \xi^{p+2}\Psi(\mu,\xi) - \xi^p\hbar_0(\mu) - \frac{\hbar_2(\mu)}{\xi^p} - \frac{\hbar_3(\mu)}{\xi^{2p}} - \ldots \quad (29)$$

By applying $\lim_{\xi\to\infty}$ to (29), we obtain

$$\hbar_1(\mu) = \lim_{\xi\to\infty}(\xi^{p+2}\Psi(\mu,\xi) - \xi^p\hbar_0(\mu)) - \lim_{\xi\to\infty}\frac{\hbar_2(\mu)}{\xi^p} - \lim_{\xi\to\infty}\frac{\hbar_3(\mu)}{\xi^{2p}} - \ldots$$

Evolute limit to derive the subsequent result:

$$\hbar_1(\mu) = \lim_{\xi\to\infty}(\xi^{p+2}\Psi(\mu,\xi) - \xi^p\hbar_0(\mu)). \quad (30)$$

Based on the consequence of Lemma 2.2, Eq. (30) is transformed as follows:

$$\hbar_1(\mu) = \lim_{\xi\to\infty}(\xi^2 A[D_\nu^p\Omega(\mu,\nu)](\xi)). \quad (31)$$

By applying Lemma 2.3 to Eq. (31), we can obtain the following:

$$\hbar_1(\mu) = D_\nu^p\Omega(\mu,0).$$

We obtain the following result by using Taylor's series and the limit:

$$\hbar_2(\mu) = \xi^{2p+2}\Psi(\mu,\xi) - \xi^{2p}\hbar_0(\mu) - \xi^p\hbar_1(\mu) - \frac{\hbar_3(\mu)}{\xi^p} - \ldots$$

A particular result is obtained by applying Lemma 2.3:

$$\hbar_2(\mu) = \lim_{\xi\to\infty}\xi^2(\xi^{2p}\Psi(\mu,\xi) - \xi^{2p-2}\hbar_0(\mu) - \xi^{p-2}\hbar_1(\mu)). \quad (32)$$

Lemmas 2.2 and 2.4 are employed to modify Eq. (32):

$$\hbar_2(\mu) = D_\nu^{2p}\Omega(\mu,0).$$

Applying the same steps as earlier, we obtain

$$\hbar_3(\mu) = \lim_{\xi\to\infty}\xi^2(A[D_\nu^{2p}\Omega(\mu,p)](\xi)).$$

Finally, we derive

$$\hbar_3(\mu) = D_\nu^{3p}\Omega(\mu,0).$$

In general,

$$\hbar_l(\mu) = D_\nu^{lp}\Omega(\mu,0).$$

This completes the proof. □

The convergence of Taylor's series is defined in the subsequent theorem.

Theorem 2.6. *For $|\xi^a A[D_\nu^{(r+1)p}\Omega(\mu,\nu)]| \le T$, the residual $R_r(\mu,\xi)$ of innovative form of MFTS validate the inequality*:

$$|R_r(\mu,\xi)| \le \frac{T}{\xi^{(r+1)p+2}}, \quad 0 < \xi \le s \quad \text{and} \quad 0 < p \le 1.$$

Proof. Let us consider that $A[D_\nu^{lp}\Omega(\mu,\nu)](\xi)$ for $l = 0, 1, 2, \ldots, r+1$, is defined on $0 < \xi \le s$. Consider that $|\xi^2 A[D_\nu^{r+1}\Omega(\mu,\mu)]| \le T$, on $0 < \xi \le s$. Let Taylor's series be

$$R_r(\mu,\xi) = \Psi(\mu,\xi) - \sum_{l=0}^{r}\frac{\hbar_l(\mu)}{\xi^{lp+2}}. \quad (33)$$

Eq. (33) is converted into the following by the application of Theorem 2.5:

$$R_r(\mu,\xi) = \Psi(\mu,\xi) - \sum_{l=0}^{r}\frac{D_\nu^{lp}\Omega(\mu,0)}{\xi^{lp+2}}. \quad (34)$$

Now, multiply $\xi^{(r+1)p+2}$ with Eq. (34):

$$\xi^{(r+1)p+2}R_r(\mu,\xi) = \xi^2(\xi^{(r+1)p}\Psi(\mu,\xi) - \sum_{l=0}^{r}\xi^{(r+1-l)p-2}D_\nu^{lp}\Omega(\mu,0)). \quad (35)$$

Lemma 2.2 is applied to Eq. (35), resulting in the following:

$$\xi^{(r+1)p+2}R_r(\mu,\xi) = \xi^2 A[D_\nu^{(r+1)p}\Omega(\mu,\nu)]. \quad (36)$$

The absolute of Eq. (36) is given as

$$|\xi^{(r+1)p+2}R_r(\mu,\xi)| = |\xi^2 A[D_\nu^{(r+1)p}\Omega(\mu,\nu)]|. \quad (37)$$

A particular result is achieved by employing the criteria specified in Eq. (37):

$$\frac{-T}{\xi^{(r+1)p+2}} \le R_r(\mu,\xi) \le \frac{T}{\xi^{(r+1)p+2}}. \quad (38)$$

Eq. (38) is also written as

$$|R_r(\mu,\xi)| \le \frac{T}{\xi^{(r+1)p+2}}.$$

Therefore, this is a particular condition for the series convergence. □

3 Methodology for the proposed model's solution

Let us consider the general PDE:

$$D_\nu^p\Omega(\mu,\nu) = \Phi(\Omega(\mu,\nu), D_\mu^\nu\Omega(\mu,\nu), D_\mu^{2\nu}\Omega(\mu,\nu), D_\mu^{3\nu}\Omega(\mu,\nu)), \quad 0 < p,\nu \le 1, \quad (39)$$

with the initial condition

$$\Omega^{(r)}(\mu,0) = h_r, \quad r = 0, 1, 2, \ldots, n-1, \quad (40)$$

where $\Omega(\mu, \nu)$ is the function which we will have to find and the operators $\Phi(\Omega(\mu, \nu), D_\mu^\nu\Omega(\mu, \nu), D_\mu^{2\nu}\Omega(\mu, \nu), D_\mu^{3\nu}\Omega(\mu, \nu))$ are linear or nonlinear of $\Omega(\mu, \nu), D_\mu^\nu\Omega(\mu, \nu), D_\mu^{2\nu}\Omega(\mu, \nu)$, and $D_\mu^{3\nu}\Omega(\mu, \nu)$.

Take the AT of Eq. (39):

$$A[\Omega(\mu, \nu)] = \frac{1}{s^p}\left[\sum_{r=0}^{n-1}\frac{\Omega^{(r)}(\mu, 0)}{s^{2-p+r}} + A[\Phi(\Omega(\mu, \nu), \times D_\mu^\nu\Omega(\mu, \nu), D_\mu^{2\nu}\Omega(\mu, \nu), D_\mu^{3\nu}\Omega(\mu, \nu))]\right], \tag{41}$$

Now, apply the inverse transformation of Aboodh:

$$\Omega(\mu, \nu) = A^{-1}\left[\frac{1}{s^p}\left[\sum_{r=0}^{n-1}\frac{\Omega^{(r)}(\mu, 0)}{s^{2-p+r}} + A[\Phi(\Omega(\mu, \nu), D_\mu^\nu\Omega(\mu, \nu), \times D_\mu^{2\nu}\Omega(\mu, \nu), D_\mu^{3\nu}\Omega(\mu, \nu))]\right]\right]. \tag{42}$$

The solution to the equation is given by an infinite series using ATIM.

$$\Omega(\mu, \nu) = \sum_{i=0}^{\infty}\Omega_i. \tag{43}$$

Decompose the operators $\Phi(\Omega, D_\mu^\nu\Omega, D_\mu^{2\nu}\Omega, D_\mu^{3\nu}\Omega)$:

$$\begin{aligned}\Phi(\Omega, D_\mu^\nu\Omega, D_\mu^{2\nu}\Omega, D_\mu^{3\nu}\Omega) &= \Phi(\Omega_0, D_\mu^\nu\Omega_0, D_\mu^{2\nu}\Omega_0, D_\mu^{3\nu}\Omega_0) \\ &+ \sum_{i=0}^{\infty}\left(\Phi\left(\sum_{r=0}^{i}(\Omega_r, D_\mu^\nu\Omega_r, D_\mu^{2\nu}\Omega_r, D_\mu^{3\nu}\Omega_r)\right)\right. \\ &\left. - \Phi\left(\sum_{r=1}^{i-1}(\Omega_r, D_\mu^\nu\Omega_r, D_\mu^{2\nu}\Omega_r, D_\mu^{3\nu}\Omega_r)\right)\right).\end{aligned} \tag{44}$$

In Eq. (42), insert (43) and (44) to obtain the result given in the following:

$$\begin{aligned}\sum_{i=0}^{\infty}\Omega_i(\mu, \nu) &= A^{-1}\left[\frac{1}{s^p}\left[\sum_{r=0}^{n-1}\frac{\Omega^{(r)}(\mu, 0)}{s^{2-p+r}} + A[\Phi(\Omega_0, D_\mu^\nu\Omega_0, D_\mu^{2\nu}\Omega_0, D_\mu^{3\nu}\Omega_0)]\right]\right] \\ &+ A^{-1}\left[\frac{1}{s^p}\left(A\left[\sum_{i=0}^{\infty}\left(\Phi\sum_{r=0}^{i}(\Omega_r, D_\mu^\nu\Omega_r, D_\mu^{2\nu}\Omega_r, D_\mu^{3\nu}\Omega_r)\right)\right]\right)\right] \\ &- A^{-1}\left[\frac{1}{s^p}\left(A\left[\left(\Phi\sum_{r=1}^{i-1}(\Omega_r, D_\mu^\nu\Omega_r, D_\mu^{2\nu}\Omega_r, D_\mu^{3\nu}\Omega_r)\right)\right]\right)\right]\end{aligned} \tag{45}$$

$$\begin{aligned}\Omega_0(\mu, \nu) &= A^{-1}\left[\frac{1}{s^p}\left(\sum_{r=0}^{n-1}\frac{\Omega^{(r)}(\mu, 0)}{s^{2-p+r}}\right)\right], \\ \Omega_1(\mu, \nu) &= A^{-1}\left[\frac{1}{s^p}(A[\Phi(\Omega_0, D_\mu^\nu\Omega_0, D_\mu^{2\nu}\Omega_0, D_\mu^{3\nu}\Omega_0)])\right], \\ &\vdots \\ \Omega_{n+1}(\mu, \nu) &= A^{-1}\left[\frac{1}{s^p}\left(A\left[\sum_{i=0}^{\infty}\left(\Phi\sum_{r=0}^{i}(\Omega_r, D_\mu^\nu\Omega_r, D_\mu^{2\nu}\Omega_r, D_\mu^{3\nu}\Omega_r)\right)\right]\right)\right] \\ &- A^{-1}\left[\frac{1}{s^p}\left(A\left[\left(\Phi\sum_{r=1}^{i-1}(\Omega_r, D_\mu^\nu\Omega_r, D_\mu^{2\nu}\Omega_r, D_\mu^{3\nu}\Omega_r)\right)\right]\right)\right],\end{aligned} \tag{46}$$

$n = 1,2, \ldots.$

The solution to Eq. (39) using ATIM is represented as follows:

$$\Omega(\mu, \nu) = \sum_{i=0}^{n-1}\Omega_i. \tag{47}$$

Example 3.1. Assume the RLW nonlinear PDE of time-fractional:

$$D_\nu^p\Omega(\mu, \nu) = \frac{\partial^3\Omega(\mu, \nu)}{\partial\nu\partial\mu^2} - \frac{1}{2}\frac{\partial\Omega^2(\mu, \nu)}{\partial\mu}, \quad \text{where } 0 < p \le 1 \tag{48}$$

with initial condition:

$$\Omega(\mu, 0) = \mu, \tag{49}$$

and exact solution

$$\Omega(\mu, \nu) = \frac{\mu}{\nu + 1}.$$

We obtain the following outcome by using the AT on either side of Eq. (48):

$$A[D_\nu^p\Omega(\mu, \nu)] = \frac{1}{s^p}\left[\sum_{r=0}^{n-1}\frac{\Omega^{(r)}(\mu, 0)}{s^{2-p+r}} + A\left[\frac{\partial^3\Omega(\mu, \nu)}{\partial\nu\partial\mu^2} - \frac{1}{2}\frac{\partial\Omega^2(\mu, \nu)}{\partial\mu}\right]\right], \tag{50}$$

We obtain the following outcome by using the AIT on either side of Eq. (50):

$$\Omega(\mu, \nu) = A^{-1}\left[\frac{1}{s^p}\left[\sum_{r=0}^{n-1}\frac{\Omega^{(r)}(\mu, 0)}{s^{2-p+r}} + A\left[\frac{\partial^3\Omega(\mu, \nu)}{\partial\nu\partial\mu^2} - \frac{1}{2}\frac{\partial\Omega^2(\mu, \nu)}{\partial\mu}\right]\right]\right]. \tag{51}$$

AT is recursively applied to obtain

$$\begin{aligned}\Omega_0(\mu,\nu) &= A^{-1}\left[\frac{1}{s^p}\left(\sum_{r=0}^{n-1}\frac{\Omega^{(r)}(\mu,0)}{s^{2-p+r}}\right)\right]\\ &= A^{-1}\left[\frac{\Omega(\mu,0)}{s^2}\right]\\ &= \mu,\end{aligned}$$

The Riemann-Liouville integral of Eq. (48) implies

$$\Omega(\mu,\nu) = \mu - A\left[\frac{\partial^3\Omega(\mu,\nu)}{\partial\nu\partial\mu^2} - \frac{1}{2}\frac{\partial\Omega^2(\mu,\nu)}{\partial\mu}\right]. \tag{52}$$

Using the ATIM process, these terms are acquired.

$$\begin{aligned}\Omega_0(\mu,\nu) &= \mu,\\ \Omega_1(\mu,\nu) &= -\frac{\mu\nu^p}{\Gamma(p+1)},\\ \Omega_2(\mu,\nu) &= \frac{\mu\nu^{2p}\left(2-\frac{\nu^p\Gamma(2p+1)^2}{\Gamma(p+1)^2\Gamma(3p+1)}\right)}{\Gamma(2p+1)},\\ \Omega_3(\mu,\nu) &= \left(\mu\nu^{4p}\left(\nu^p\left(-\frac{\nu^{2p}\Gamma(2p+1)^2\Gamma(6p+1)}{\Gamma(7p+1)} + \frac{\sqrt{\pi}4^{1-3p}\nu^p\Gamma(p+1)^2\Gamma(5p+1)}{\Gamma\left(3p+\frac{1}{2}\right)}\right.\right.\right.\\ &\quad\left.\left.\left. - \frac{2\Gamma(p+1)\Gamma(3p+1)(2\Gamma(3p+1)\Gamma(p+1)^3+\Gamma(2p+1)^3)\Gamma(4p+1)}{\Gamma(2p+1)^2\Gamma(5p+1)}\right) + \frac{\pi^{3/2}4^{1-4p}\Gamma(p+1)\Gamma(3p+1)^3}{\Gamma\left(p+\frac{1}{2}\right)^2\Gamma\left(2p+\frac{1}{2}\right)}\right)\right.\\ &\quad /(\Gamma(p+1)^4\Gamma(3p+1)^2).\end{aligned} \tag{53}$$

The ATIM gives this final solution:

$$\Omega(\mu,\nu) = \Omega_0(\mu,\nu) + \Omega_1(\mu,\nu) + \Omega_2(\mu,\nu) + \Omega_3(\mu,\nu) + \ldots \tag{54}$$

$$\begin{aligned}\Omega(\mu,\nu) &= \mu - \frac{\mu\nu^p}{\Gamma(p+1)} + \frac{\mu\nu^{2p}\left(2-\frac{\nu^p\Gamma(2p+1)^2}{\Gamma(p+1)^2\Gamma(3p+1)}\right)}{\Gamma(2p+1)} + \left(\mu\nu^{4p}\left(\nu^p\left(-\frac{\nu^{2p}\Gamma(2p+1)^2\Gamma(6p+1)}{\Gamma(7p+1)}\right.\right.\right.\\ &\quad\left.\left. + \frac{\sqrt{\pi}4^{1-3p}\nu^p\Gamma(p+1)^2\Gamma(5p+1)}{\Gamma\left(3p+\frac{1}{2}\right)} - \frac{2\Gamma(p+1)\Gamma(3p+1)(2\Gamma(3p+1)\Gamma(p+1)^3+\Gamma(2p+1)^3)\Gamma(4p+1)}{\Gamma(2p+1)^2\Gamma(5p+1)}\right)\right.\\ &\quad\left. + \frac{\pi^{3/2}4^{1-4p}\Gamma(p+1)\Gamma(3p+1)^3}{\Gamma\left(p+\frac{1}{2}\right)^2\Gamma\left(2p+\frac{1}{2}\right)}\right)\Big/(\Gamma(p+1)^4\Gamma(3p+1)^2) + \ldots.\end{aligned} \tag{55}$$

Example 3.2. Consider the fractional-order GRLW nonlinear PDE:

$$\begin{aligned}D_\nu^p\Omega(\mu,\nu) &= \frac{\partial^3\Omega(\mu,\nu)}{\partial\nu\partial\mu^2} - \Omega(\mu,\nu)\frac{\partial\Omega(\mu,\nu)}{\partial\mu}\\ &\quad - \frac{\partial\Omega(\mu,\nu)}{\partial\mu}, \quad \text{where} \quad 0 < p \le 1\end{aligned} \tag{56}$$

Having IC's:

$$\Omega(\mu,0) = 3k\,\mathrm{sech}^2(l\mu), \tag{57}$$

and exact solution

$$\Omega(\mu,\nu) = 3k\,\mathrm{sech}^2(l(\mu-(1-k)\nu)).$$

We obtain the following outcome by using the AT on either side of Eq. (56):

$$A[D_v^p\Omega(\mu,v)] = \frac{1}{s^p}\left(\sum_{r=0}^{n-1}\frac{\Omega^{(r)}(\mu,0)}{s^{2-p+r}} + A\left[\frac{\partial^3\Omega(\mu,v)}{\partial v\partial\mu^2} - \Omega(\mu,v)\frac{\partial\Omega(\mu,v)}{\partial\mu} - \frac{\partial\Omega(\mu,v)}{\partial\mu}\right]\right), \tag{58}$$

We obtain the following outcome by using the AIT on either side of Eq. (58):

$$\Omega(\mu,v) = A^{-1}\left[\frac{1}{s^p}\left(\sum_{r=0}^{n-1}\frac{\Omega^{(r)}(\mu,0)}{s^{2-p+r}} + A\left[\frac{\partial^3\Omega(\mu,v)}{\partial v\partial\mu^2} - \Omega(\mu,v)\frac{\partial\Omega(\mu,v)}{\partial\mu} - \frac{\partial\Omega(\mu,v)}{\partial\mu}\right]\right)\right]. \tag{59}$$

The iterative procedure of the AT is used to derive this equation:

$$\begin{aligned}\Omega_0(\mu,v) &= A^{-1}\left[\frac{1}{s^p}\left(\sum_{r=0}^{n-1}\frac{\Omega^{(r)}(\mu,0)}{s^{2-p+r}}\right)\right]\\ &= A^{-1}\left[\frac{\Omega(\mu,0)}{s^2}\right]\\ &= 3k\,\mathrm{sech}^2(l\mu).\end{aligned}$$

The Riemann-Liouville integral of Eq. (56) implies:

$$\Omega(\mu,v) = 3k\,\mathrm{sech}^2(l\mu) - A\left[\frac{\partial^3\Omega(\mu,v)}{\partial v\partial\mu^2} - \Omega(\mu,v)\frac{\partial\Omega(\mu,v)}{\partial\mu} - \frac{\partial\Omega(\mu,v)}{\partial\mu}\right]. \tag{60}$$

These terms are obtained using the ATIM process:

$$\begin{aligned}\Omega_0(\mu,v) &= 3k\,\mathrm{sech}^2(l\mu),\\ \Omega_1(\mu,v) &= \frac{3klv^p\tanh(l\mu)\,\mathrm{sech}^4(l\mu)(6k+\cosh(2l\mu)+1)}{\Gamma(p+1)},\\ \Omega_2(\mu,v) &= \frac{3}{2}kl^2v^{2p}\,\mathrm{sech}^6(l\mu)\left(\frac{-252k^2\,\mathrm{sech}^2(l\mu)+(48k-2)\cosh(2l\mu)+72k(3k-1)+\cosh(4l\mu)-3}{\Gamma(2p+1)}\right.\\ &\quad\left.+\frac{3kl4^pv^p\Gamma\left(p+\frac{1}{2}\right)\tanh(l\mu)\,\mathrm{sech}^4(l\mu)(6k+\cosh(2l\mu)+1)((24k-2)\cosh(2l\mu)-36k+\cosh(4l\mu)-3)}{\sqrt{\pi}\,\Gamma(p+1)\Gamma(3p+1)}\right).\end{aligned} \tag{61}$$

The ATIM gives this final solution:

$$\Omega(\mu,v) = \Omega_0(\mu,v) + \Omega_1(\mu,v) + \Omega_2(\mu,v) + \ldots \tag{62}$$

$$\begin{aligned}\Omega(\mu,v) &= 3k\,\mathrm{sech}^2(l\mu) + \frac{3klv^p\tanh(l\mu)\,\mathrm{sech}^4(l\mu)(6k+\cosh(2l\mu)+1)}{\Gamma(p+1)}\\ &\quad+\frac{3}{2}kl^2v^{2p}\,\mathrm{sech}^6(l\mu)\left(\frac{-252k^2\,\mathrm{sech}^2(l\mu)+(48k-2)\cosh(2l\mu)+72k(3k-1)+\cosh(4l\mu)-3}{\Gamma(2p+1)}\right.\\ &\quad\left.+\frac{3kl4^pv^p\Gamma\left(p+\frac{1}{2}\right)\tanh(l\mu)\,\mathrm{sech}^4(l\mu)(6k+\cosh(2l\mu)+1)((24k-2)\cosh(2l\mu)-36k+\cosh(4l\mu)-3)}{\sqrt{\pi}\,\Gamma(p+1)\Gamma(3p+1)}\right)\\ &\quad+\ldots.\end{aligned} \tag{63}$$

Example 3.3. Consider the fractional-order RLW nonlinear PDE:

$$D_v^p\Omega(\mu,v) = 2\frac{\partial^3\Omega(\mu,v)}{\partial v\partial\mu^2} - \frac{\partial\Omega(\mu,v)}{\partial\mu}, \quad \text{where } 0 < p \le 1 \tag{64}$$

Having ICs:

$$\Omega(\mu,0) = e^{-\mu} \tag{65}$$

and exact solution

$$\Omega(\mu,v) = e^{v-\mu},$$

we obtain the following outcome using the AT on either side of Eq. (64):

$$A[D_v^p\Omega(\mu,v)] = \frac{1}{s^p}\left(\sum_{r=0}^{n-1}\frac{\Omega^{(r)}(\mu,0)}{s^{2-p+r}} + A\left[2\frac{\partial^3\Omega(\mu,v)}{\partial v\partial\mu^2} - \frac{\partial\Omega(\mu,v)}{\partial\mu}\right]\right), \tag{66}$$

We obtain the following outcome by using the AIT on either side of (66):

$$\Omega(\mu,v) = A^{-1}\left[\frac{1}{s^p}\left(\sum_{r=0}^{n-1}\frac{\Omega^{(r)}(\mu,0)}{s^{2-p+r}} + A\left[2\frac{\partial^3\Omega(\mu,v)}{\partial v\partial\mu^2} - \frac{\partial\Omega(\mu,v)}{\partial\mu}\right]\right)\right]. \tag{67}$$

The following is the equation that results from applying the AT iteratively:

$$\begin{aligned}\Omega_0(\mu,\nu) &= A^{-1}\left[\frac{1}{s^p}\left(\sum_{r=0}^{n-1}\frac{\Omega^{(r)}(\mu,0)}{s^{2-p+r}}\right)\right]\\ &= A^{-1}\left[\frac{\Omega(\mu,0)}{s^2}\right]\\ &= e^{-\mu},\end{aligned}$$

The Riemann–Liouville integral of Eq. (64) implies

$$\Omega(\mu,\nu) = e^{-\mu} - A\left[2\frac{\partial^3\Omega(\mu,\nu)}{\partial\nu\partial\mu^2} - \frac{\partial\Omega(\mu,\nu)}{\partial\mu}\right]. \tag{68}$$

The following terms may be acquired by using the ATIM procedure:

$$\begin{aligned}\Omega_0(\mu,\nu) &= e^{-\mu},\\ \Omega_1(\mu,\nu) &= \frac{e^{-\mu}\nu^p}{\Gamma(p+1)},\\ \Omega_2(\mu,\nu) &= \frac{e^{-\mu}\nu^{2p}}{\Gamma(2p+1)},\\ \Omega_2(\mu,\nu) &= \frac{e^{-\mu}\nu^{3p}}{\Gamma(3p+1)}.\end{aligned} \tag{69}$$

The ATIM gives this final solution:

$$\Omega(\mu,\nu) = \Omega_0(\mu,\nu) + \Omega_1(\mu,\nu) + \Omega_2(\mu,\nu) + \Omega_3(\mu,\nu) + \ldots. \tag{70}$$

$$\Omega(\mu,\nu) = \frac{e^{-\mu}\nu^{2p}}{\Gamma(2p+1)} + \frac{e^{-\mu}\nu^{3p}}{\Gamma(3p+1)} + \frac{e^{-\mu}\nu^{p}}{\Gamma(p+1)} + e^{-\mu} + \ldots. \tag{71}$$

Example 3.4. Consider the fractional-order RLW nonlinear PDE:

$$D_\nu^p\Omega(\mu,\nu) = -\frac{\partial^4\Omega(\mu,\nu)}{\partial\mu^4}, \quad \text{where} \quad 0 < p \le 1, \tag{72}$$

Having ICs:

$$\Omega(\mu,0) = \sin(\mu) \tag{73}$$

and exact solution

$$\Omega(\mu,\nu) = e^{-\nu}\sin(\mu).$$

We obtain the following outcome by using the AT on either side of Eq. (72):

$$A[D_\nu^p\Omega(\mu,\nu)] = \frac{1}{s^p}\left(\sum_{r=0}^{n-1}\frac{\Omega^{(r)}(\mu,0)}{s^{2-p+r}} + A\left[-\frac{\partial^4\Omega(\mu,\nu)}{\partial\mu^4}\right]\right). \tag{74}$$

We obtain the following outcome by using the AIT on either side of (74):

$$\Omega(\mu,\nu) = A^{-1}\left[\frac{1}{s^p}\left(\sum_{r=0}^{n-1}\frac{\Omega^{(r)}(\mu,0)}{s^{2-p+r}} + A\left[-\frac{\partial^4\Omega(\mu,\nu)}{\partial\mu^4}\right]\right)\right]. \tag{75}$$

The following is the equation that results from applying the AT iteratively:

$$\begin{aligned}\Omega_0(\mu,\nu) &= A^{-1}\left[\frac{1}{s^p}\left(\sum_{r=0}^{n-1}\frac{\Omega^{(r)}(\mu,0)}{s^{2-p+r}}\right)\right]\\ &= A^{-1}\left[\frac{\Omega(\mu,0)}{s^2}\right]\\ &= \sin(\mu).\end{aligned}$$

The Riemann–Liouville integral of Eq. (72) implies

$$\Omega(\mu,\nu) = \sin(\mu) - A\left[-\frac{\partial^4\Omega(\mu,\nu)}{\partial\mu^4}\right]. \tag{76}$$

The following terms may be acquired by using the ATIM procedure:

$$\begin{aligned}\Omega_0(\mu,\nu) &= \sin(\mu),\\ \Omega_1(\mu,\nu) &= -\frac{\nu^p\sin(\mu)}{\Gamma(p+1)},\\ \Omega_2(\mu,\nu) &= \frac{\nu^{2p}\sin(\mu)}{\Gamma(2p+1)},\\ \Omega_2(\mu,\nu) &= -\frac{\nu^{3p}\sin(\mu)}{\Gamma(3p+1)}.\end{aligned} \tag{77}$$

Table 1: Analysis of different p values of ATIM solution and its comparison with VHPTM [37] and VIM [24] for $\nu = 0.1$

μ	ATIM$_{p=0.64}$	ATIM$_{p=0.84}$	ATIM$_{p=1.00}$	Exact	ATIM Error$_{p=1.00}$	VIM Error$_{p=1.00}$	*VHPTM* Error$_{p=1.00}$
0.1	0.0975762	0.0993929	0.0999001	0.0999001	6.661672×10^{-11}	1.000000×10^{-10}	1.000000×10^{-10}
0.2	0.1951520	0.1987860	0.1998000	0.1998000	1.332334×10^{-10}	2.000000×10^{-10}	2.000000×10^{-10}
0.3	0.2927290	0.2981790	0.2997000	0.2997000	1.998501×10^{-10}	3.000000×10^{-10}	3.000000×10^{-10}
0.4	0.3903050	0.3975720	0.3996000	0.3996000	2.664669×10^{-10}	4.000000×10^{-10}	4.000000×10^{-10}
0.5	0.4878810	0.4969640	0.4995000	0.4995000	3.330836×10^{-10}	5.000000×10^{-10}	5.000000×10^{-10}
0.6	0.5854570	0.5963570	0.5994010	0.5994010	3.997003×10^{-10}	6.000000×10^{-10}	6.000000×10^{-10}
0.7	0.6830340	0.6957500	0.6993010	0.6993010	4.663169×10^{-10}	7.000000×10^{-10}	7.000000×10^{-10}
0.8	0.7806100	0.7951430	0.7992010	0.7992010	5.329338×10^{-10}	8.000000×10^{-10}	8.000000×10^{-10}
0.9	0.8781860	0.8945360	0.8991010	0.8991010	5.995504×10^{-10}	9.000000×10^{-10}	9.000000×10^{-10}
1.	0.9757620	0.9939290	0.9990010	0.9990010	6.661672×10^{-10}	10.00000×10^{-9}	10.00000×10^{-9}

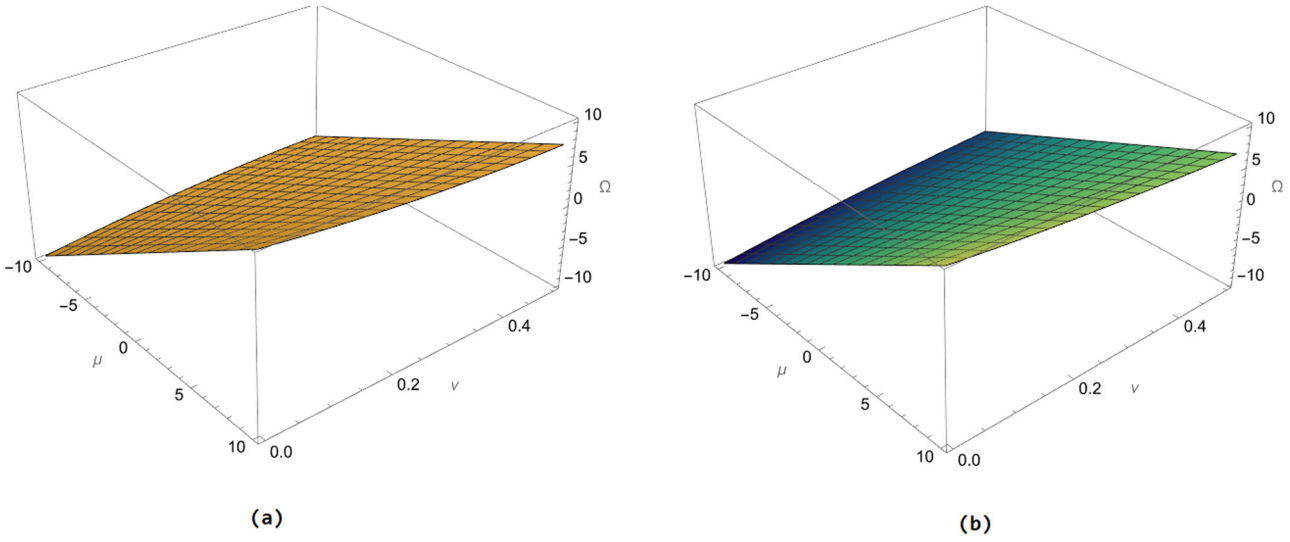

Figure 1: Comparison among exact solution (a) and approximate solution (b) for $p = 1$.

The ATIM gives this final solution:

$$\Omega(\mu, \nu) = \Omega_0(\mu, \nu) + \Omega_1(\mu, \nu) + \Omega_2(\mu, \nu) + \Omega_3(\mu, \nu) + \ldots. \tag{78}$$

$$\Omega(\mu, \nu) = \frac{\nu^{2p} \sin(\mu)}{\Gamma(2p+1)} - \frac{\nu^{3p} \sin(\mu)}{\Gamma(3p+1)} - \frac{\nu^{p} \sin(\mu)}{\Gamma(p+1)} + \sin(\mu) + \ldots. \tag{79}$$

4 Graphical discussion

The study systematically employs the iterative transform method (ATIM) to explore fractional RLW equations, particularly focusing on ion-acoustic plasma waves. The results derived from the analysis are visualized and compared through various figures and tables, offering clear insights into the dynamics of plasma waves under different parameter settings.

Table 1 provides a comparative analysis of different p-values for the ATIM solution against the VHPTM and VIM methods, for $\nu = 0.1$ in Example 1. This table illustrates how ATIM fares in terms of accuracy compared to other established methods, highlighting its efficacy. Figure 1 presents a visual comparison between the exact solution and the approximate ATIM solution for $p = 1$ in Example 1. This figure helps in understanding the approximation's closeness to the exact solution, validating the method's reliability. Figure 2 (a and b) shows the effect of varying p-values on the solution for $\nu = 0.1$ in both 3D and 2D

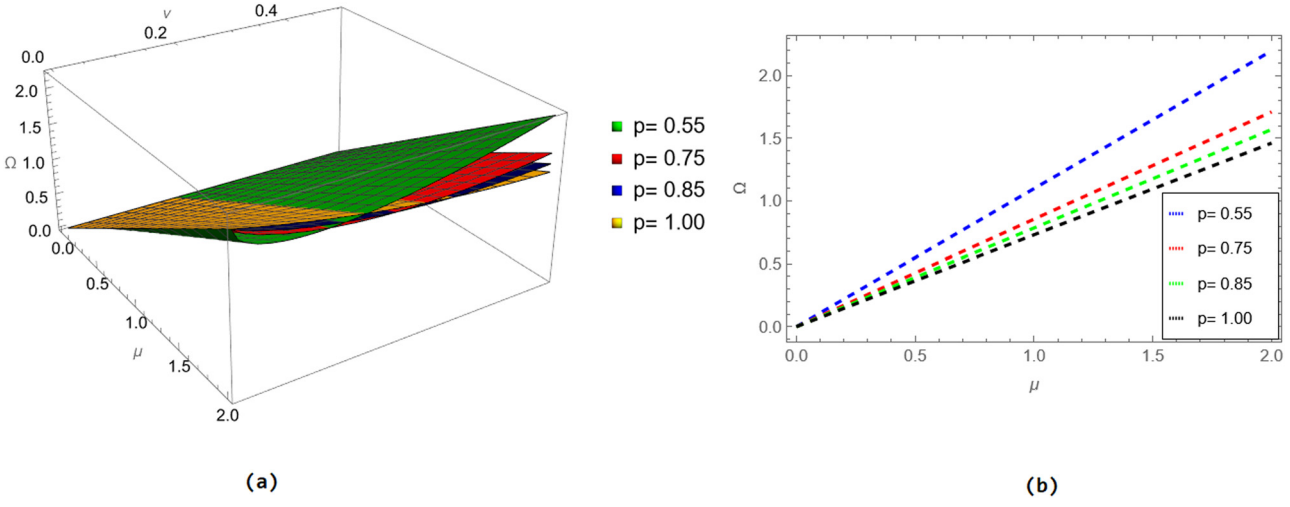

Figure 2: (a and b) Effect of p values on the solution for $\nu = 0.1$, in 3D and 2D, respectively.

Table 2: Effect of p values on ATIM solution of the model

μ	$\text{ATIM}_{p=0.64}$	$\text{ATIM}_{p=0.84}$	$\text{ATIM}_{p=1.00}$	Exact	$\text{Error}_{p=1.00}$
0.1	1.49636	1.49626	1.49626	1.49626	1.492190×10^{-7}
0.2	1.48531	1.48511	1.48510	1.48510	2.938261×10^{-7}
0.3	1.46705	1.46677	1.46675	1.46675	4.294912×10^{-7}
0.4	1.44196	1.44159	1.44157	1.44156	5.524302×10^{-7}
0.5	1.41049	1.41005	1.41002	1.41002	6.596072×10^{-7}
0.6	1.37324	1.37274	1.37271	1.37271	7.488684×10^{-7}
0.7	1.33086	1.33031	1.33028	1.33028	8.189984×10^{-7}
0.8	1.28409	1.28350	1.28346	1.28346	8.697005×10^{-7}
0.9	1.23366	1.23304	1.23300	1.23300	9.015113×10^{-7}
1.	1.18034	1.17971	1.17967	1.17967	9.156672×10^{-7}

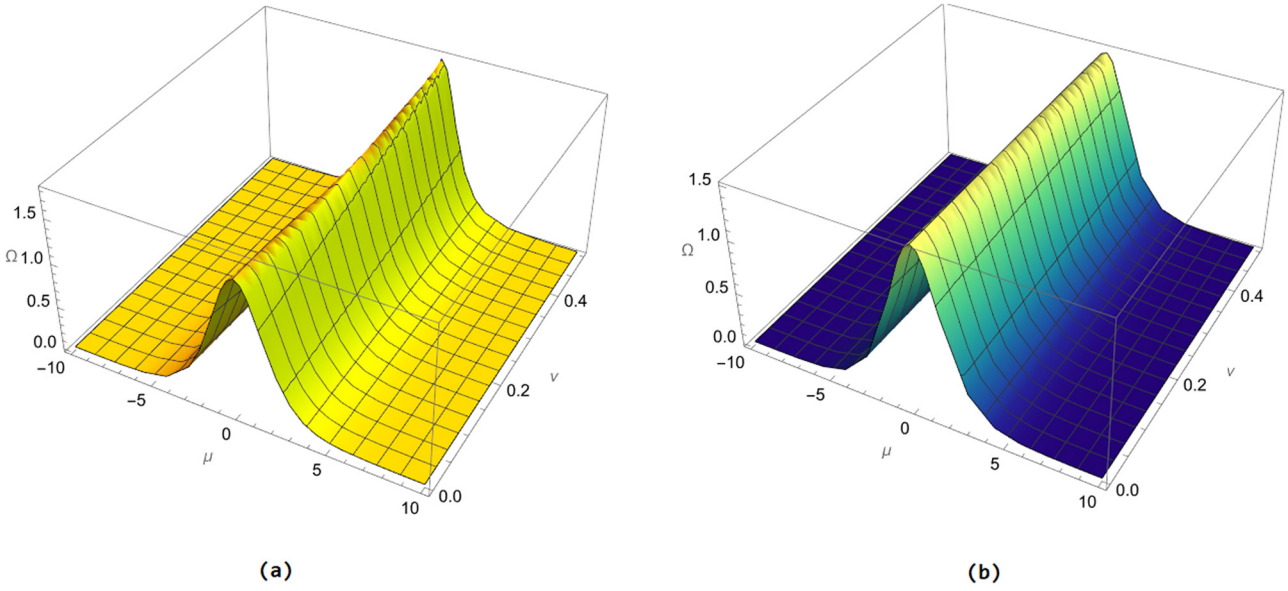

Figure 3: Comparison among exact solution (a) and approximate solution (b) for $p = 1$.

perspectives in Example 1. These visualizations depict how the changes in p-values influence the behavior of the solution, emphasizing the sensitivity of the plasma wave model to parameter variations. Table 2 focuses on how p-values affect the ATIM solution of the model in Example 2. This helps in quantifying the impact of varying parameters on the solution accuracy. Figure 3 compares the exact and approximate solutions for $p = 1$ in Example 2, similar to Figure 1, further validating the ATIM approach for different examples. Figure 4 (a and b) similarly illustrates the effect of different p-values on the solution for $\nu = 0.1$ in 3D and 2D, showing the dynamics of the plasma waves as influenced by these values in Example 2. Table 3 provides an analysis for different p-values in Example 3, comparing the ATIM solution against VHPTM and HPSTM methods for $\nu = 0.0000001$. This highlights the robustness of ATIM in handling small values of $\nu = 0.0000001$. Figure 5 compares the exact and approximate solutions for $p = 1$ in Example 3, reaffirming the accuracy of ATIM under different conditions. Figure 6 (a and b) displays the effect of varying p-values on the solution for $p = 1$ in 3D and 2D, showing the sensitivity of solutions to these parameter changes. Table 4 presents the effect of p-values on the ATIM solution for the general model, offering a numerical perspective to the findings. Figure 7 visually compares the exact and approximate solutions for $p = 1$, summarizing the approximation capabilities of ATIM. Figure 8 (a and b) illustrates the effect of p-values on the solution for $\nu = 0.1$ in 3D and 2D, reinforcing the significance of the parameter variations on the plasma wave dynamics. These figures and tables collectively demonstrate the efficacy of ATIM in capturing the dynamics of fractional ion-acoustic plasma waves, providing

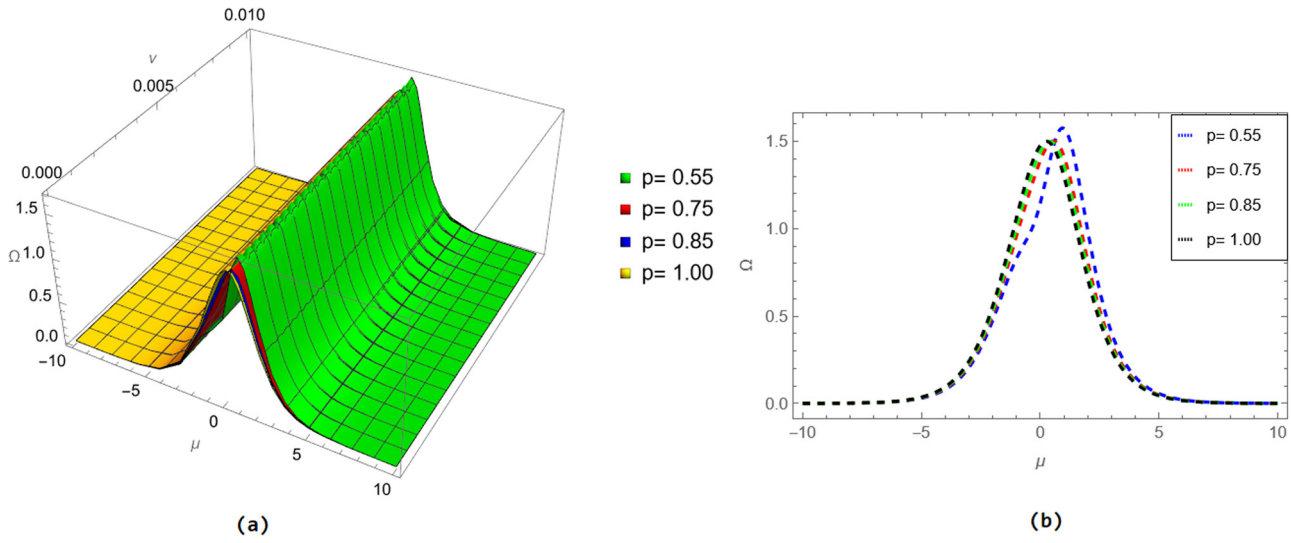

Figure 4: (a and b) Effect of p values on the solution for $\nu = 0.1$, in 3D and 2D, respectively.

Table 3: Analysis of different p values of ATIM solution and its comparison with VHPTM [37] and HPSTM [15] for $\nu = 0.0000001$

μ	$\text{ATIM}_{p=0.64}$	$\text{ATIM}_{p=0.84}$	$\text{ATIM}_{p=1.00}$	Exact	$\text{ATIM Error}_{p=1.00}$	$\text{HPSTM Error}_{p=1.00}$	$\text{VHPTM Error}_{p=1.00}$
0.1	0.928067	0.910395	0.905743	0.905743	3.774758×10^{-14}	8.396197×10^{-9}	9.100000×10^{-10}
0.2	0.839750	0.823760	0.819550	0.819550	3.419486×10^{-14}	2.343247×10^{-9}	8.200000×10^{-9}
0.3	0.759837	0.745369	0.741559	0.741559	3.075317×10^{-14}	1.098518×10^{-8}	7.400000×10^{-9}
0.4	0.687529	0.674437	0.670991	0.670991	2.786659×10^{-14}	2.435301×10^{-8}	6.700000×10^{-9}
0.5	0.622102	0.610256	0.607137	0.607137	2.531308×10^{-14}	3.925301×10^{-8}	6.100000×10^{-9}
0.6	0.562901	0.552183	0.549361	0.549361	2.287059×10^{-14}	5.222691×10^{-8}	5.500000×10^{-9}
0.7	0.509334	0.499636	0.497082	0.497082	2.070565×10^{-14}	6.061930×10^{-8}	5.000000×10^{-9}
0.8	0.460864	0.452089	0.449779	0.449779	1.876276×10^{-14}	6.351737×10^{-8}	4.500000×10^{-9}
0.9	0.417007	0.409067	0.406976	0.406976	1.698641×10^{-14}	6.159048×10^{-8}	4.100000×10^{-9}
1.	0.377324	0.370139	0.368248	0.368248	1.532107×10^{-14}	5.612475×10^{-8}	3.700000×10^{-9}

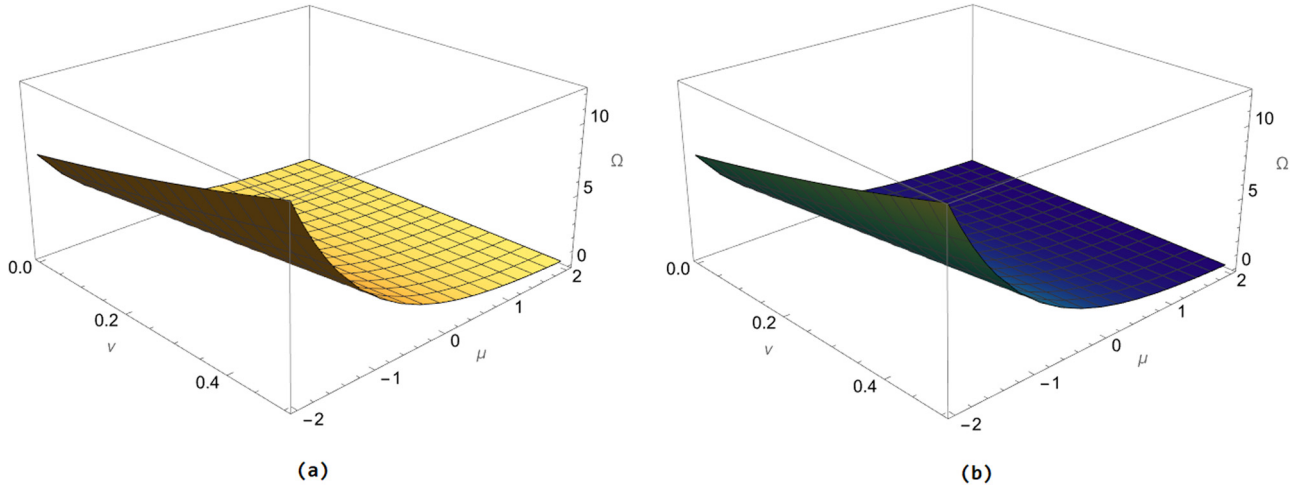

Figure 5: Comparison among exact solution (a) and approximate solution (b) for $p = 1$.

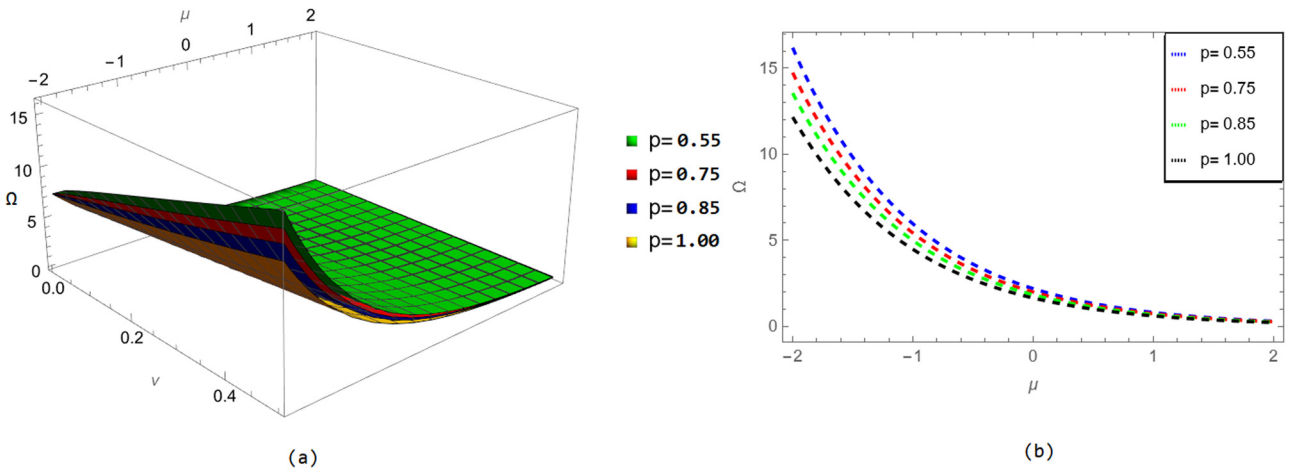

Figure 6: (a and b) Effect of p values on the solution for v = 0.0000001, in 3D and 2D, respectively.

Table 4: Effect of p values on ATIM solution of the model

μ	$\text{ATIM}_{p=0.64}$	$\text{ATIM}_{p=0.84}$	$\text{ATIM}_{p=1.00}$	Exact	$\text{Error}_{p=1.00}$
0.1	0.0914801	0.0964722	0.0988401	0.0988401	4.151420×10^{-11}
0.2	0.182046	0.191981	0.196693	0.196693	8.261361×10^{-11}
0.3	0.270793	0.285571	0.29258	0.29258	1.228875×10^{-10}
0.4	0.356835	0.376307	0.385544	0.385544	1.619336×10^{-10}
0.5	0.439311	0.463284	0.474655	0.474655	1.993618×10^{-10}
0.6	0.517398	0.545632	0.559024	0.559024	2.347979×10^{-10}
0.7	0.590315	0.622528	0.637808	0.637808	2.678881×10^{-10}
0.8	0.657333	0.693204	0.710218	0.710218	2.983016×10^{-10}
0.9	0.717784	0.756954	0.775533	0.775533	3.257345×10^{-10}
1.	0.771063	0.813141	0.833098	0.833098	3.499128×10^{-10}

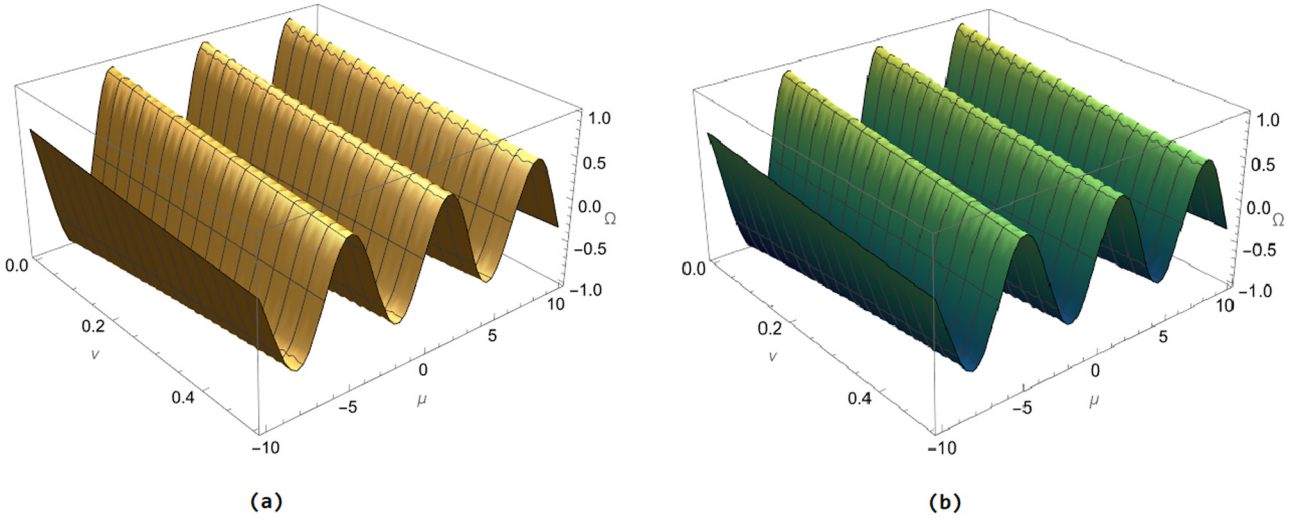

Figure 7: Comparison among exact solution (a) and approximate solution (b) for p = 1.

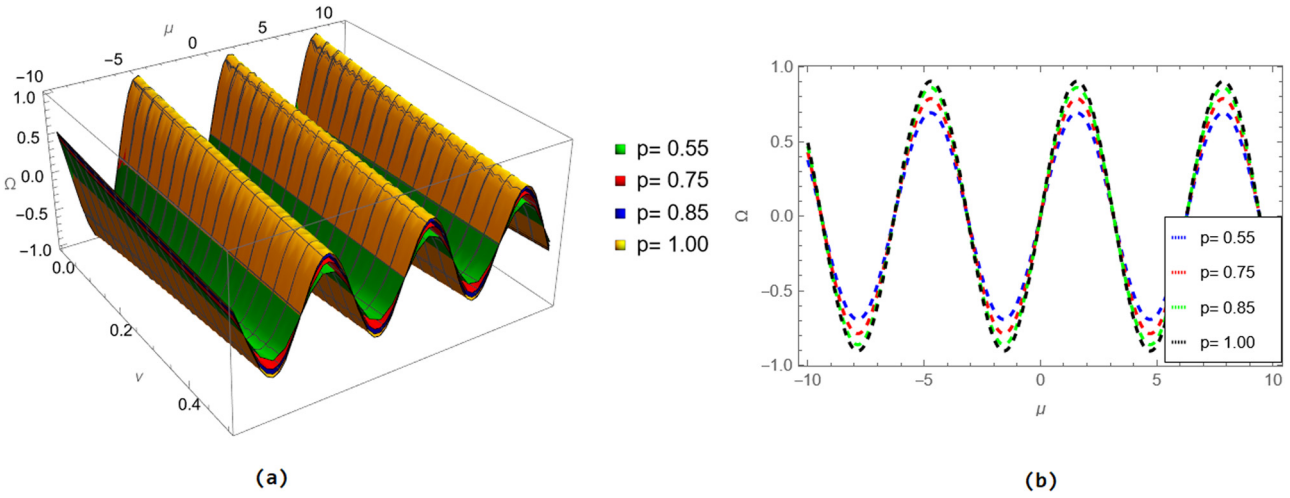

Figure 8: (a and b) Effect of p values on the solution for $\nu = 0.1$, in 3D and 2D, respectively.

both numerical and visual evidence of the method's reliability and potential for broader applications in solving fractional-order wave equations.

5 Conclusion

We have studied the fractional generalized form of the RLW equation using the Caputo derivative to describe the ion-acoustic of the salty plasma. Using the ITM led us to approximate solutions and helped to investigate the effect of fractional-order derivatives on wave propagation. Although ITM is an established for analytical methods, our research illustrates the influence of fractional calculus onto plasma wave behavior through a comparison between integer-order and fractional-order models. These findings indicate that fractional derivatives lead to changes in wave dispersion and stability, presenting a new perspective for analyzing intricate plasma behavior. While there is still no consensus on the interpretation of memory in plasma systems, it is well established that fractional models can accurately describe nonlocal interactions and anomalous diffusion. This demonstrates the accuracy of fractional modeling and gives more support to the significance of fractional-order in theoretical plasma physics because it encourages the applications of fractional-order to the system of collisional plasma.

Acknowledgments: The authors acknowledge the funding by the Scientific Research Deanship at the University of Ha'il, Saudi Arabia, through the Project Number: RG-23 059.

Funding information: This research was funded by the Scientific Research Deanship at the University of Ha'il, Saudi Arabia, through the Project Number: RG-23 059.

Author contributions: All authors have accepted responsibility for the entire content of this manuscript and approved its submission. Naveed Iqbal, Mohammad Alqudah, Yousef Jawarneh, Ahmad Shafee, Ali M. Mahnashi, and Fazal Ghani Conceptualization, methodology, software, validation, formal analysis, investigation, resources, data curation, writing – original draft preparation, writing – review and editing, visualization, supervision, project administration. All authors have read and agreed to the published version of the manuscript.

Conflict of interest: The authors state no conflict of interest.

Data availability statement: The datasets generated and/or analysed during the current study are available from the corresponding author on reasonable request.

References

[1] Debnath L. Recent applications of fractional calculus to science and engineering. Int J Math Math Sci. 2003;2003:3413–42.
[2] Meerschaert MM, Tadjeran C. Finite difference approximations for two-sided space-fractional partial differential equations. Appl Numer Math. 2006;56(1):80–90.
[3] Parvizi M, Eslahchi MR, Dehghan M. Numerical solution of fractional advection-diffusion equation with a nonlinear source term. Numer Algor. 2015;68:601–29.

[4] Bu W, Liu X, Tang Y, Yang J. Finite element multigrid method for multi-term time fractional advection diffusion equations. Int J Model Simulat Sci Comput. 2015;6(1):1540001.
[5] Baleanu D, Jajarmi A, Mohammadi H, Rezapour S. A new study on the mathematical modelling of human liver with Caputo-Fabrizio fractional derivative. Chaos Solitons Fractals. 2020;134:109705.
[6] Tuan NH, Mohammadi H, Rezapour S. A mathematical model for COVID-19 transmission by using the Caputo fractional derivative. Chaos Solitons Fractals. 2020;140:110107.
[7] Lin XL, Ng MK, Sun HW. A multigrid method for linear systems arising from time-dependent two-dimensional space-fractional diffusion equations. J Comput Phys. 2017;336:69–86.
[8] Chavez-Vazquez S, Lavin-Delgado JE, Gomez-Aguilar JF, Razo-Hernandez JR, Etemad S, Rezapour S. Trajectory tracking of Stanford robot manipulator by fractional-order sliding mode control. Appl Math Model. 2023;120:436–462.
[9] Mohammadi H, Kumar S, Rezapour S, Etemad S. A theoretical study of the Caputo-Fabrizio fractional modeling for hearing loss due to Mumps virus with optimal control. Chaos Solitons Fractals. 2021144:110668.
[10] Baleanu D, Aydogn SM, Mohammadi H, Rezapour S. On modelling of epidemic childhood diseases with the Caputo-Fabrizio derivative by using the Laplace Adomian decomposition method. Alexandria Engineering Journal, 2020;59(5):3029–39.
[11] Khan H, Alam K, Gulzar H, Etemad S, Rezapour S. A case study of fractalfractional tuberculosis model in China: Existence and stability theories along with numerical simulations. Mathematics and Computers in Simulation. 2022;198:455–73.
[12] Baleanu D, Etemad S, Mohammadi H, Rezapour S. A novel modeling of boundary value problems on the glucose graph. Communications in Nonlinear Science and Numerical Simulation. 2021;100:105844.
[13] Shah R, Khan H, Kumam P, Arif M. An analytical technique to solve the system of nonlinear fractional partial differential equations. Mathematics, 2019;7(6):505.
[14] Khan H, Shah R, Baleanu D, Kumam P, Arif M. Analytical solution of fractionalorder hyperbolic telegraph equation, using natural transform decomposition method. Electronics. 2019;8(9):1015.
[15] Goswami A, Singh J, Kumar D, Gupta S. An efficient analytical technique for fractional partial differential equations occurring in ion acoustic waves in plasma. J Ocean Eng Sci. 2019;4(2):85–99.
[16] Almatrafi MB. Abundant traveling wave and numerical solutions for Novikov-Veselov system with their stability and accuracy. Appl Anal. 2023;102(8):2389–402.
[17] Almatrafi MB, Alharbi A. New soliton wave solutions to a nonlinear equation arising in plasma physics. CMES-Comput Model Eng Sci. 2023;137(1):827.
[18] Alharbi AR, Almatrafi MB. Exact solitary wave and numerical solutions for geophysical KdV equation. J King Saud Univ-Sci. 2022;34(6):102087.
[19] Almatrafi MB. Solitary wave solutions to a fractional model using the improved modified extended tanh-function method. Fractal Fract. 2023;7(3):252.
[20] Almatrafi MB. Construction of closed form soliton solutions to the space-time fractional symmetric regularized long wave equation using two reliable methods. Fractals. 2023;31(10):2340160.
[21] Khan Y, Taghipour R, Falahian M, Nikkar A. A new approach to modified regularized long wave equation. Neural Comput Appl. 2013;23:1335–41.
[22] Peregrine DH. Calculations of the development of an undular bore. J Fluid Mech. 1966;25(2):321–30.
[23] Benjamin TB, Bona JL, Mahony JJ. Model equations for long waves in nonlinear dispersive systems. Philos Trans R Soc London. Ser A Math Phys Sci. 1972;272(1220):47–78.
[24] Ganji DD, Tari H, Jooybari MB. Variational iteration method and homotopy perturbation method for nonlinear evolution equations. Comput Math Appl. 2007;54(7–8):1018–27.
[25] Dag I. Least-squares quadratic B-spline finite element method for the regularized long wave equation. Comput Meth Appl Mech Eng. 2000;182(1–2):205–15.
[26] Khalifa AK, Raslan KR, Alzubaidi H. Numerical study using ADM for the modified regularized long wave equation. Appl Math Model. 2008;32(12):2962–72.
[27] Achouri T, Omrani K. Numerical solutions for the damped generalized regularized long-wave equation with a variable coefficient by Adomian decomposition method. Commun Nonl Sci Numer Simulat. 2009;14(5):2025–33.
[28] Inc M, Ugurlu Y. Numerical simulation of the regularized long wave equation by He's homotopy perturbation method. Phys Lett A. 2007;369(3):173–9.
[29] Ojo GO, Mahmudov NI. Aboodh transform iterative method for spatial diffusion of a biological population with fractional-order. Mathematics. 2021;9(2):155.
[30] Awuya MA, Ojo GO, Mahmudov NI. Solution of space-time fractional differential equations using Aboodh transform iterative method. J Math. 2022;2022:14.
[31] Awuya MA, Subasi D. Aboodh transform iterative method for solving fractional partial differential equation with Mittag-Leffler Kernel. Symmetry. 2021;13(11):2055.
[32] Aboodh KS. New integral transform Aboodh transform. Global J Pure Appl Math. 2013;9(1):35–43.
[33] Aggarwal S, Chauhan R. A comparative study of Mohand and Aboodh transforms. Int J Res Advent Tech. 2019;7(1):520–9.
[34] Benattia ME, Belghaba K. Application of the Aboodh transform for solving fractional delay differential equations. Univ J Math Appl. 2020;3(3):93–101.
[35] Delgado BB, Macias-Diaz JE. On the general solutions of some non-homogeneous Div-curl systems with Riemann-Liouville and Caputo fractional derivatives. Fractal Fract. 2021;5(3):117.
[36] Alshammari S, Al-Smadi M, Hashim I, Alias MA. Residual power series technique for simulating fractional Bagley-Torvik problems emerging in applied physics. Appl Sci. 2019;9(23):5029.
[37] Ali I, Khan H, Shah R, Baleanu D, Kumam P, Arif M. Fractional view analysis of acoustic wave equations, using fractional-order differential equations. Appl Sci. 2020;10(2):610.